

Received January 12, 2022, accepted February 24, 2022, date of publication March 8, 2022, date of current version March 17, 2022.

Digital Object Identifier 10.1109/ACCESS.2022.3157340

# Spectrum Allocation Techniques for Cognitive Radio Networks

MARAM HELMY<sup>1</sup>, MOHAMED S. HASSAN<sup>1</sup>, AND MAHMOUD H. ISMAIL<sup>1,2</sup>, (Senior Member, IEEE)

<sup>1</sup>Department of Electrical Engineering, American University of Sharjah, Sharjah, United Arab Emirates

<sup>2</sup>Department of Electronics and Communications Engineering, Faculty of Engineering, Cairo University, Giza 12613, Egypt

Corresponding author: Mohamed S. Hassan (mshassan@aus.edu)

This work was supported in part by the American University of Sharjah OAP Program OAPCEN-1410-E00055.

**ABSTRACT** The remarkable growth in the demand for multimedia streaming over wireless networks is challenged by spectrum scarcity. To mitigate the effect of such a challenge, Cognitive Radio Networks (CRNs) were introduced as a promising technology since CRNs offer a great advantage to unlicensed users, also known as secondary users (SUs), by allowing them to opportunistically access the licensed bands when these bands are not used by their primary users (PUs). In this work, an LTE-based CRN is proposed with the objective of guaranteeing continuous video playback at the SUs end at acceptable perceptual quality. To accomplish this objective, different resource allocation schemes are introduced to adaptively assign the available channels to SUs while considering the quality of these channels as well as the buffer occupancies of the different SUs. In addition, a streaming algorithm is proposed to ensure the delivery of the base and enhancement layers of the scalable video frames within the delay constraints with priority given to the base-layers of the video frames to guarantee the continuity of video playback. Furthermore, adaptive modulation is used based on the channel state information (CSI) as fed-back by the SUs. The performance of the proposed schemes is evaluated through extensive Monte-Carlo simulations.

**INDEX TERMS** Cognitive radio networks, Markov chains, primary radio user activity, resource allocation, LTE.

## I. INTRODUCTION

Over the past few years, the demand for bandwidth-hungry applications (e.g., Netflix, Youtube, etc.) has been exponentially growing. These applications have generated the majority of traffic in wireless and wired networks over the last decade [1] and is expected to account for 82% of traffic in 2022 [2]. Therefore, despite the recent advances in wireless technology, multimedia applications will continue their increase in the demand for more bandwidth. As a result, the expected growth in wireless multimedia applications will always be challenged by their stringent quality-of-service (QoS) requirements in addition to the expected shortage of the radio spectrum, also known as the spectrum scarcity problem. However, it was argued in [3] that spectrum scarcity is not mainly due to shortage in the availability of the resources, but due to how they are licensed and how they are utilized, which is usually caused by the static assignment of the licensed

spectrum. Recent measurements have generally shown that only less than 5% of the statically assigned spectrum is efficiently used [4], [5]. To improve spectrum utilization, the concept of opportunistic access of the available spectrum was first presented in [6]. This is also known as dynamic spectrum access (DSA) where an unlicensed user, also called secondary user (SU), is allowed to access the unused or idle bands of the licensed spectrum of the licensed or primary users (PUs) [3]. When a PU is absent from a particular frequency band (i.e., idle) at distinct points in time and space, this is known as a spectrum hole [7]. Specifically, a spectrum hole is a reserved segment of the spectrum that is idle. A recently introduced technology that is expected to help to overcome the scarcity problem is cognitive radio (CR), which is a DSA technique that efficiently uses the spectrum and hence can help in satisfying the growing demand for innovative wireless services.

This inspired many researchers to propose different schemes with the objective of enabling dynamic allocation of inefficiently utilized spectrum to SUs in need. Therefore,

The associate editor coordinating the review of this manuscript and approving it for publication was Mohammad S. Khan.

Cognitive Radio Networks (CRNs) were introduced as a promising solution for efficient spectrum utilization by enabling interactive wireless users to sense and learn the surrounding environment and correspondingly adapt their transmission strategies [8].

The nature of bandwidth-hungry multimedia applications allows them to become one of the candidates that can fully benefit from the many potentials of CRNs. The main challenge of video streaming over a CRN is to maintain stable and optimal video quality under the time-varying nature of the underlying wireless channels. Recently, CRNs have been considered to be the future of the cellular networks in the context of spectrum sharing between different operators. Spectrum sharing allows a lightly loaded operator to share their unused spectrum with another operator to achieve efficient spectrum utilization. This is relevant in the context of the 4G cellular standard 3GPP LTE-A due to the recently introduced feature of carrier aggregation (CA) [9], [10]. The LTE is a technology that offers high spectral efficiency, fast adaptation to time-varying channel conditions and robustness against interference [11], [12] and more importantly spectrum flexibility. Such advantageous characteristics resulted in choosing LTE as the implementation platform of CRNs. The authors in [9] suggested the use of sensing for dynamic spectrum sharing in cognitive LTE-A cellular networks. They developed and analyzed energy detectors that were designed to solve the problem of sensing in the presence of a desired signal in an LTE-A based system. Also, the target of the work in [13] was to implement a spatial interweave LTE-TDD based cognitive radio. The authors argued that using LTE as the physical layer of the CRN would result in an increase of the network spectral efficiency. In addition, they focused on spatial interweave CRNs in which a SU uses an antenna array to perform null-beamforming in the PU's direction in order to spatially reuse the spectrum. They also proposed innovative solutions to avoid interference to the primary system where an over-the-air calibration technique at the secondary base station was designed in addition to a beamforming strategy based on the channel reciprocity hypothesis inherent in TDD systems. Furthermore, the authors in [14] proposed a CR-based coordinated dynamic spectrum access scheme for LTE, where a Spectrum Policy Server (SPS) is responsible for spectrum management in an LTE multi-operator heterogeneous network (HetNet). They stated that their proposed architecture improved the spectral efficiency and thus achieved enhanced data rates. The work in [12] investigated the allocation of transmission power and bandwidth in a cognitive LTE based network that contains a secondary enhanced NodeBs (eNBs) with different signal-to-interference-plus-noise (SINR) requirements in addition to different application-layer quality-of-service (QoS) requirements. A novel resource allocation strategy was proposed in which the total queue size in the eNBs at the PUs and SUs is minimized subject to interference requirement and queue stability constraints of the primary eNBs. Their proposed

algorithm showed low complexity and outperformed previously proposed schemes.

Generally, resource allocation is a key mechanism in deciding on the optimal assignment of the available resources among different SUs such that the performance of the CRN is optimized. Such optimization could be based on some criteria such as maximizing the throughput, fairness, spectral efficiency [15]. However, a fundamental requirement of CRNs is that the SUs should not cause any interference to the PUs. Nevertheless, the nature and requirements of the underlying applications over CRN should still be taken into consideration when assigning CRN resources. Therefore, in what follows, we shed light on the requirements of video streaming applications and common techniques in the literature for resource allocation in CRNs. In [16], [17], the authors focused on streaming scalable encoded video-on-demand over CRNs in an infrastructure-based CR system. They proposed a channel allocation scheme that jointly considers the status of the playback buffers at the SUs and the quality of the available channels while allocating channels among active SUs. They also presented an adaptive video streaming algorithm that employs Scalable Video Coding (SVC) while adapting the modulation level based on the channel conditions with the objective of meeting a target bound on the achieved bit error rate (BER). Also, in [18], a content driven proportionate channel allocation scheme for streaming SVC over CRNs was proposed. It takes into consideration the various requirements of secondary applications while maintaining the long term fairness among SUs. The main aim of the work was to improve the overall satisfaction of the SUs by increasing the quality-of-experience (QoE) especially for rapid motion (RM) type of video users. The work in [19] investigated the problem of multicast multimedia streaming in multi-hop CRNs and proposed an intelligent multicast routing protocol for multi-hop ad hoc CRNs that can support multimedia streaming. The proposed protocol performs path selection and channel assignment for the different multi-cast receivers. Path selection is based on the shortest path tree (SPT) that performs the expected transmission count metric (ETX). Channel selection is based on the ETX, which is a function of the probability of success (POS) over the different channels, which, in turn, depends on the channel-quality and availability. In [20], the authors proposed a heuristic channel allocation mechanism to lower the complexity of their obtained optimization problem, which is of order  $\mathcal{O}(n^3)$ , where  $n$  is the number of the active SUs in the network. The proposed algorithm randomly selects a PU and a SU at each iteration. During each iteration, the selected SU scans the selected primary channel to gather information about the transmission power of the PU and channel status. Assuming that the number of PUs is less than the SUs, after some iterations, all the primary channels will be scanned and thus the SUs can select their channels. In [21], the problem of resource allocation was formulated as an Integer Linear Programming (ILP) problem where a heuristic scheme was proposed to solve this ILP problem.

The idea of the scheme is to divide the available bands into  $M$  sets and each SU forms a preferable channel list for the other SUs. Based on the distance from other users and the SINR of the channel, channels with lower SINR will be assigned to the closest users.

The performance of CRNs is highly dependent on efficient modeling of the PUs' behavior. Several models have been proposed in the literature. For example, the authors in [8] and [22] modeled the traffic patterns of PUs using an  $M/G/1$  queue model in which arrivals are Markovian, service times have a general distribution, and the packet arrival process is a Poisson random process with average packet arrival rate  $\lambda$ . While [23]–[26] assumed that the activity of a PU follows the Poisson model, however, [27] argued that such a model neglects the short-term fluctuations as well as the bursty and spiky features of the PU activities. Thus, a first-difference filter clustering model was proposed to overcome the drawbacks of the Poisson model. Another approach that is widely used in the literature is the Markovian based model. For example, the work done in [28]–[30] used continuous- and discrete-time Markov chains (MC) models. A special case is the 2-state MC model where there are only two states, namely, the busy state, which is the state when the radio channel is occupied by the PU, and the idle state, which is the state when the radio channel is free and a SU can opportunistically access the channel. By the same token, in [31]–[37], the PU activity pattern in each channel was assumed to be a continuous ON/OFF random process where the ON-period represents the time when a PU channel is busy i.e., occupied by one of the PUs, and the OFF-period represents the time where a PU channel is idle. The ON/OFF periods are assumed to be exponentially distributed with parameters  $\lambda_{\text{ON}}$  and  $\lambda_{\text{OFF}}$ , respectively.

In this work, we consider a CRN over an LTE platform. This CRN consists of  $N$  PUs and  $M$  SUs where it is assumed that the activity pattern of the PU follows the widely accepted 2-state continuous-time MC model. In this model, state 1 indicates that the PU is idle and thus the corresponding channel can be used by any of the SUs. Similarly, state 0 implies that the PU' channel is busy and thus, cannot be allocated to any SU in demand for a channel. It is also assumed that the PU channels switch from state 1 to 0 and from state 0 to 1 with exponential rates, respectively. The objective is to guarantee uninterrupted video playback at the SUs with acceptable perceptual quality. To achieve such an objective, various resource allocation schemes are introduced. These schemes adaptively allocate the idle PU channels to SUs while considering the quality of their assigned channels in addition to their buffer occupancies. Furthermore, a streaming algorithm is introduced to guarantee the delivery of scalable video frames. Specifically, this algorithm aims to deliver the base and enhancement layers within the delay constraints with higher priority granted to the base-layers to ensure the continuity of video playback. Additionally, adaptive modulation is employed while taking into considerations the channel state information (CSI) as fed-back by the

reporting SUs. Extensive Monte-Carlo simulations are used to evaluate the performance of the proposed schemes.

The rest of the paper is organized as follows. In Section II, the system model and problem formulation are introduced. The proposed dynamic resource allocation algorithms are introduced in Section III. Numerical and simulation results are discussed in Section IV before the paper is finally concluded in Section V.

## II. SYSTEM MODEL

In this work, we consider a CR system over an LTE platform, where  $N$  SUs denoted by  $SU_1, \dots, SU_N$  share a set of  $M$  orthogonal primary channels denoted by  $PU_1, \dots, PU_M$  each with  $K$  resource blocks (RBs), which are denoted by  $RB_1, \dots, RB_K$ . This system assumes an interweave mode of transmission such that the PUs and SUs cannot simultaneously access the CR spectrum. Therefore, once a channel is declared idle by the base station (BS), it will remain available until the end of a certain period of time denoted by  $T_{\text{slot}}$ . In this model, RBs are scheduled every transmit time interval (TTI), which is set to 1 ms. In addition, the proposed model adopts equal power allocation to guarantee that the same transmission power is allocated to all RBs. In this case, this allocated power is equal to the maximum power assigned to the BS divided by the total number of RBs [38]–[40]. This system model is illustrated in Fig. 1. The behavior of any of the PU channels is modeled by the discrete 2-state MC shown in Fig. 2 with a transition probability matrix  $P_m$  where each of the states represents whether the  $m$ -th channel,  $m \in \{1, 2, \dots, M\}$ , is available or not. When in the "Idle" state, the  $m$ -th PU channel is available and can be allocated to any of the SUs, while when in the "Busy" state, the  $m$ -th PU channel can not be allocated to any of the SUs. The CR base station (CR-BS) allows the opportunistic access of the available PU channels through efficient spectrum sensing and channel assignment of any available PU channels among the SUs. Spectrum sensing [41] and management [9] are extensively addressed in the literature and therefore are beyond the scope of this work. Moreover, it is assumed that the  $N$  SUs are interested in streaming video sequences via the CR-BS from a video source hosting video sequences that are scalable-encoded using the H.264/SVC standard and can be rate controlled without the need for transcoding.

The idle (i.e. available) PU channels are allocated to the active SUs based on the information they feedback to the streaming algorithm. This includes the instantaneous buffer occupancies of the SUs as well as the signal-to-noise ratio (SNR) of the available PU channels as measured by interested SUs. The channel gain  $h_{\text{BS,SU}}$  is assumed to be constant within each TTI. The micro urban channel model introduced in [42] is adopted in this work. Additionally, shadow and Rayleigh fading are also assumed in this work. The log-normal random distribution is used to model the shadow fading whereas the path loss for the BS-SU link is defined as  $36.7 \log_{10}(d[\text{m}]) + 22.7 + 26 \log_{10}(f[\text{GHz}])$ . The duration of an idle time slot  $T_{\text{slot}}$  is assumed to be fixed

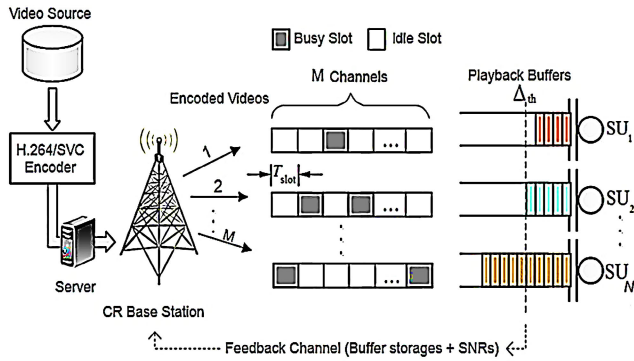


FIGURE 1. Proposed video streaming scenario.

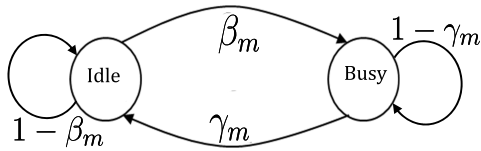


FIGURE 2. Primary user channel model.

and equal to one TTI. In this work, it is assumed that each available channel can only serve one user every TTI, however, a SU can be assigned more than one PU channel based on availability and on the current requirements and reported information by other SUs. Once a channel is declared idle, the CR-BS schedules the transmission of video frames under the constraints of a maximum bit budget of each of the allocated channels while meeting the delay deadline according to the proposed channel allocation and streaming algorithms as will be explained later.

Prior to channel allocation, the buffer occupancies as well as channel state information (CSI) are reported by the SUs to the CR-BS. Based on this reported information, the CR-BS estimates the number of RBs required by the  $n$ -th SU using the following metric:

$$RB_n^{\text{Req}} = \frac{\bar{r}_n}{\frac{1}{N} \sum_{j=1}^N \bar{r}_j} \times \frac{R_n^{\text{req}}}{\frac{1}{N} \sum_{j=1}^N R_j^{\text{req}}}, \quad (1)$$

where  $R_n^{\text{req}}$  is the required throughput of the  $n$ -th SU and  $\bar{r}_n$  is defined as

$$\bar{r}_n = \frac{1}{K} \sum_{i=1}^R \text{SNR}_{n,i}, \quad (2)$$

where  $\text{SNR}_{n,i}$  is the SNR of the  $n$ -th SU on the  $i$ -th RB over a specific TTI. The achievable rate of any user is then assumed to be calculated using the well-known Shannon's capacity formula.

### III. PROPOSED DYNAMIC RESOURCE ALLOCATION ALGORITHMS

The goal of the proposed algorithms is to maintain the continuity of the video playback at the SUs end while guaranteeing the quality of the streamed scalable video sequences.

Therefore, the channel allocation algorithms are designed to sense and identify available PU channels then adaptively allocate the RBs at these PU channels to the SUs based on their reported information, which is periodically received every  $T_{\text{slot}}$ . In this work, it is assumed that the CR-BS always gets the feedback information from the SUs before the next transmission (i.e., during  $T_{\text{slot}}$ ) on a reliable error-free reverse channel. This information includes the buffer occupancy of the SU as well as the measured SNR on the different channels from that SU's perspective. Three resource allocation schemes are proposed and investigated in terms of their performance. The pseudocodes for the proposed resource allocation algorithms are explained in what follows in Algorithms 1, 2, and 3, respectively.

#### A. BUFFER-BASED ALLOCATION

The first allocation strategy is solely based on the status of the playback buffer as detailed in Algorithm 1. In more details, available RBs are allocated to the SUs by the the BS. This is done based on a comparison of their buffer occupancies to a predefined threshold,  $\Delta_{th}$ , to decide on the urgency of sending the video frames to each of the SUs. Thus, the SUs with lower occupancies are served first to avoid starvation, however, they may not be allocated a good quality RBs. Therefore, this Buffer-Based algorithm considers the following two scenarios:

- All SUs have their buffer occupancies larger than the threshold ( $\Delta_n > \Delta_{th}, \forall n = 1, 2, \dots, N$ ), or all their buffer occupancies are below or equal the threshold ( $\Delta_n \leq \Delta_{th}, \forall n = 1, 2, \dots, N$ ). In this case, the available RBs are equally allocated to the SUs in a Round Robin fashion, starting with the SU with the minimum occupancy. The procedure is repeated until all the available RBs are fully allocated to the SUs.
- Some SUs are underflowing ( $\Delta_n \leq \Delta_{th}, n = 1, 2, \dots, N_u$ ) with  $N_u \leq N$ . Thus, the available RBs are only allocated to the SUs in need starting with the SU of the minimum occupancy and so on. The procedure is repeated until all the available RBs are allocated in full to the SUs.

#### B. SNR-BASED ALLOCATION

The second allocations scheme is solely based on the reported SNR of the different RBs as seen by the SUs as detailed in Algorithm 2. Each SU reports to the BS a vector of the measured SNRs over all the available RBs,  $\text{SNR}_n = [\text{SNR}_{n,1}, \text{SNR}_{n,2}, \dots, \text{SNR}_{n,K}], \forall n = 1, 2, \dots, N$ . To elaborate, assume that the  $n^{\text{th}}$  SU has the largest SNR reported for the  $k^{\text{th}}$  RB, thus,  $\text{SNR}_{k,n} = \max(\text{SNR}_{k,1}, \text{SNR}_{k,2}, \dots, \text{SNR}_{k,N})$ . Hence, the BS will allocate the  $k^{\text{th}}$  RB to the  $n^{\text{th}}$  user who can achieve the maximum quality when assigned that RB. When two or more SUs have the same quality level for on the same RB, this RB is allocated randomly to any of them. However, it is important to note that allocation that is only based on reported SNRs

**Algorithm 1: Buffer-Based Allocation**

**Input** :  $K, \Delta_n, RB_n^{Req}, n = 1, 2, \dots, N$   
**Output**:  $RB_{SU_1}, RB_{SU_2}, \dots, RB_{SU_N}$  // Vector of RBs allocated to each SU.  
**Set** :  $\Delta_{th} = x$ ; // Buffer threshold.  
1 **if**  $\Delta_n > \Delta_{th}$  or  $\Delta_n \leq \Delta_{th}, \forall n = 1, 2, \dots, N$  **then**  
2      $sort(\Delta_1, \Delta_2, \dots, \Delta_N)$  // sort in the ascending order.  
   Allocate required RBs to all SUs on Round Robin basis;  
3      $K \leftarrow K - RB_n^{Req}$  // the remaining available RBs  
4 **end if**  
5 **else if**  $\Delta_n \leq \Delta_{th}, n = 1, 2, \dots, N_u$  **then**  
6      $sort(\Delta_1, \Delta_2, \dots, \Delta_{N_u})$  // sort in the ascending order. Allocate required RBs to all SUs on Round Robin basis;  
7      $K \leftarrow K - RB_n^{Req}$  // the remaining available RBs  
8 **end if**

may assign the RBs with good quality to SUs that are not starving while ignoring those in need. Clearly, when the state of the playback buffer is ignored, this may result in starvation instants and hence interruptions in the playback for some of the SUs. As before, the procedure is repeated until all the available RBs are fully allocated to the SUs.

**Algorithm 2: SNR-Based Allocation**

**Input** :  $K, SNR_n, n = 1, 2, \dots, N, RB_n^{Req}$ .  
**Output**:  $RB_{SU_1}, RB_{SU_2}, \dots, RB_{SU_N}$  // Vector of RBs allocated to each SU.  
1 **for**  $k = 1, 2, \dots, K$  // for each available RB **do**  
2      $SNR_{k,n} = \max(SNR_{k,1}, SNR_{k,2}, \dots, SNR_{k,N})$ ; //  
   Allocate the required RBs to  $SU_n$  with max SNR  
3      $K \leftarrow K - RB_n^{Req}$  // the remaining available RBs  
4      $SNR_{(:,n)} = 0$  // remove  $SU_n$   
5 **end for**

**C. JOINT BUFFER AND SNR BASED ALLOCATION**

The third allocation scheme is a joint one in which allocation is based on both the channel quality and playback buffer occupancy as detailed in Algorithm 3 and Fig. 3. The BS allocates SUs with buffer occupancies below the threshold ( $\Delta_n$ ) the available RBs on channels with the highest SNR. Such a strategy is expected to reduce the possibility of any needed retransmissions and hence results in efficient utilization of the available resources while maintaining uninterrupted video playback at acceptable quality.

**D. PROPOSED STREAMING ALGORITHM**

The streaming algorithm is responsible for scheduling of the video frames within the slots of the allocated RBs based on certain constraints, which, for example, could be frames deadlines to guarantee continuous playback. In this work,

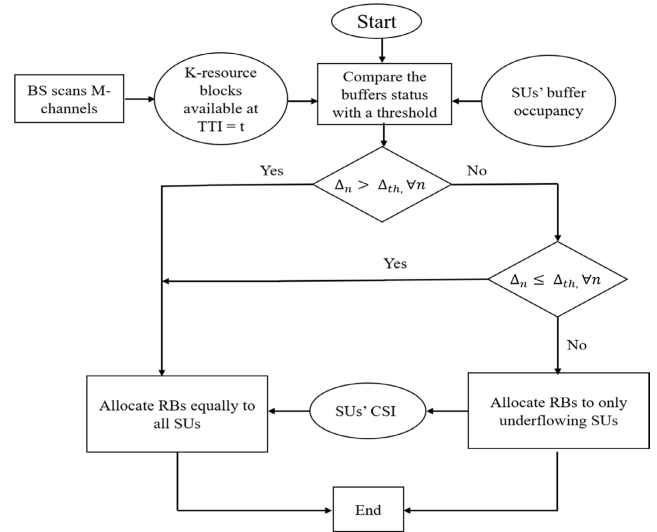


**FIGURE 3. Joint buffer and SNR based allocation algorithm flow chart.**

**Algorithm 3: Joint Buffer and SNR Based Allocation**

**Input** :  $K, SNR_n, n = 1, 2, \dots, N, RB_n^{Req}$ .  
**Output**:  $RB_{SU_1}, RB_{SU_2}, \dots, RB_{SU_N}$  // Vector of RBs allocated to each SU.  
**Set** :  $\Delta_{th} = x$ ; // Buffer threshold.  
1 **if**  $\Delta_n > \Delta_{th}$  or  $\Delta_n \leq \Delta_{th}, \forall n = 1, 2, \dots, N$  **then**  
2      $sort(\Delta_1, \Delta_2, \dots, \Delta_N)$  // sort in the ascending order.  
   Allocate the required RBs to all SUs on Round Robin basis;  
3     **for**  $k = 1, 2, \dots, K$  // for each available RB. **do**  
4          $SNR_{k,n} = \max(SNR_{k,1}, SNR_{k,2}, \dots, SNR_{k,N})$ ;  
       Allocate the required RBs to  $SU_n$  with max SNR;  
5          $K \leftarrow K - RB_n^{Req}$  // the remaining available RBs  
6          $SNR_{(:,n)} = 0$  // remove  $SU_n$   
7     **end for**  
8 **end if**  
9 **else if**  $\Delta_n \leq \Delta_{th}, n = 1, 2, \dots, N_u$  **then**  
10      $sort(\Delta_1, \Delta_2, \dots, \Delta_{N_u})$  // sort in the ascending order.  
   Allocate RB to only in need SUs on Round Robin basis according to their ascending order;  
11     **for**  $k = 1, 2, \dots, K$  // for each available RB. **do**  
12          $SNR_{k,n} = \max(SNR_{k,1}, SNR_{k,2}, \dots, SNR_{k,N_u})$ ;  
       Allocate required RBs to  $SU_n$  with max SNR;  
13          $K \leftarrow K - RB_n^{Req}$  // the remaining available RBs  
14          $SNR_{(:,n)} = 0$  // remove  $SU_n$   
15     **end for**  
16 **end if**

video sequences are encoded using the H.264/SVC encoding standard into one base layer (BL) and two enhancement layers (ELs). It is well known that receiving only the BLs provides the basic acceptable quality level, however, the quality level can be enhanced by guaranteeing the correct transmission

of more ELs. If the buffer occupancy of a SU is below the desired threshold, then the BL of the video sequence of that SU is transmitted for the purpose of maintaining the playback continuity. After the successful transmission of all scheduled BLs of the SUs, the streaming algorithm checks whether there is still available RBs or not. If yes, then the algorithm schedules the transmission of more ELs to further improve the achieved quality. To decide which EL layers to transmit, the number of layers  $L$  of a frame  $f$  should be received before the deadline of that frame. This is done by adding the current time slot  $t$  to the time required to transmit ELs using

$$t + \frac{\sum_{l=1}^L b_n^{f,l}}{\bar{r}_n} < \text{display time of frame } f, \quad (3)$$

where  $b_n^{f,l}$  is the number of bits in the  $l^{\text{th}}$  EL of frame  $f$  and  $\bar{r}_n$  is the average rate of the  $n^{\text{th}}$  SU.

#### IV. SIMULATION RESULTS

In this section, we provide the details of the simulation setup and results to study, compare and validate the proposed allocation and streaming strategies. For the simulation environment, we used MATLAB and all numerical results are averaged over 50 simulation runs where each run lasts for 30 seconds. In all simulations, the BS transmits encoded video sequences to  $N = \{3, 8, 15\}$  SUs over  $M = 3$  PUs' channels that are opportunistically accessed according to the discrete-time two-state Markov chain model with transition matrix

$$P = \begin{pmatrix} 0.957 & 0.043 \\ 0.9 & 0.1 \end{pmatrix} \quad (4)$$

with limiting probability  $\pi_1 = 0.3$ . Moreover, in our simulations, we consider a single LTE cell with a BS located at the center of the cell with a radius of 500 m and a number of downlink RBs =  $\{6 - 100\}$ . PUs and SUs are distributed randomly in the cell. Available RBs are uniformly distributed among the PU channels by the BS. For example, if the BS operates at 20 MHz, there will be 100 RBs available, in total, to be distributed among the 3 PUs. Clearly, the total number of RBs available for SUs depends on the number of available (i.e., idle) PU channels. For instance, if there is only one idle PU channel, then 33 RBs are available, if 2 PU channels are idle then 66 RBs are available, and so on. Finally, according to the LTE standard, the transmission power of the BS is set to the maximum value of 46 dBm (39.8 W).

##### A. STREAMING SINGLE-LAYERED VIDEO

In this work, the trace file for the single layer H.264 encoded Sony Demo video sequence with a playback rate of  $f_p = 30$  fps and a group of picture (GoP) structure of G16B15 is used. A main objective of this study is to maintain continuous playback at the SUs end by preventing/limiting starvation instants at the playback buffer by providing SUs in need with channels of the best possible quality while guaranteeing fairness among the SUs. To evaluate the performance of the proposed allocation schemes, two metrics are applied: the

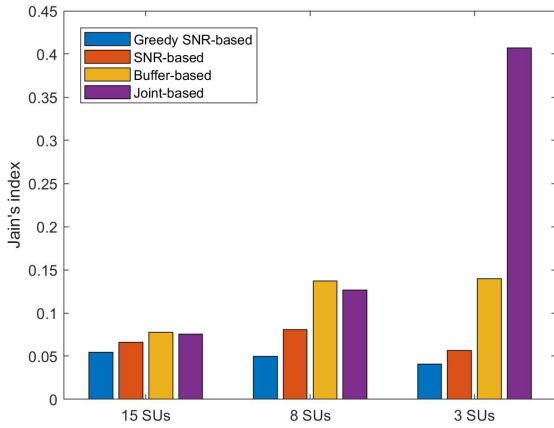
average buffer occupancy of each of the SUs and the Jain's fairness index. The Jain's fairness index is a metric used in network engineering to determine fairness among users. The result ranges from  $\frac{1}{N}$  (worst case) to 1 (best case). The Jain's fairness index is calculated using

$$J(R_{SU_1}, R_{SU_2}, \dots, R_{SU_N}) = \frac{(\sum_{i=1}^N R_{SU_i})^2}{N \times \sum_{i=1}^N (R_{SU_i})^2}. \quad (5)$$

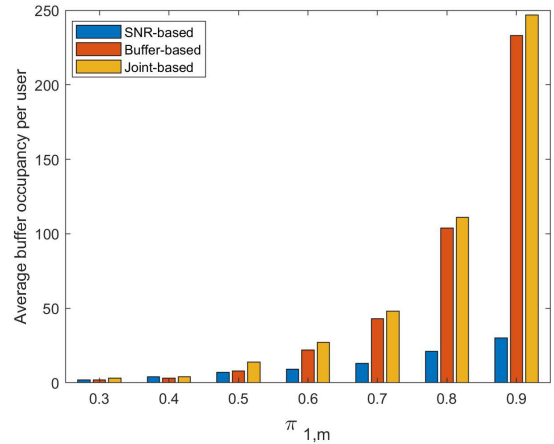
Figure 4 shows the Jain's fairness index calculated using (5) for different numbers of RBs and different numbers of SUs for the proposed allocation strategies. For the SNR-based allocation, two scenarios are considered and labeled in the figure as greedy SNR and SNR-based allocation, respectively. The difference between the two techniques is that in the greedy SNR approach, SUs reporting the highest SNR during the different TTIs will be always allocated the available RBs. However, in the SNR-based technique, the SUs in need could be assigned RBs only once in every TTI. Intuitively, the greedy SNR approach is the worst in terms of fairness for all cases and thus is not recommended. Whereas, the joint buffer and SNR-based technique outperforms the other approaches in terms of fairness as the number of SUs decreases. Such behaviors are depicted in Figs. 4(a), 4(b) and 4(c). Figure 4 also shows that the buffer-based allocation technique has comparable performance to the joint and SNR-based approaches as the number of SUs increases and the number of RBs decreases.

Figures 5(a), 5(b) and 5(c) show the effect of the steady state (i.e., limiting) probability of finding a channel (say the  $m$ -th channel) idle (i.e.,  $\pi_{1,m}$ ) on the average buffer occupancy per user. In this figure, the number of RBs is fixed to 6 for a different numbers of SUs  $\{3, 8, 15\}$ . It can be seen that the joint buffer and SNR-based approach outperforms the SNR-based and buffer-based, when deployed individually, in most of the cases. Also, the figure shows another intuitive result, which is as the number of SUs increases, the average number of frames at the SUs' buffers decreases. Such behavior is expected since the fixed shared resources are now distributed among a higher number of users. Also, it is noticed that as  $\pi_{1,m}$  increases, the average number of frames at the SUs' buffers increases. This is expected since a higher number of video frames could be transmitted as the probability of having more idle channels increases.

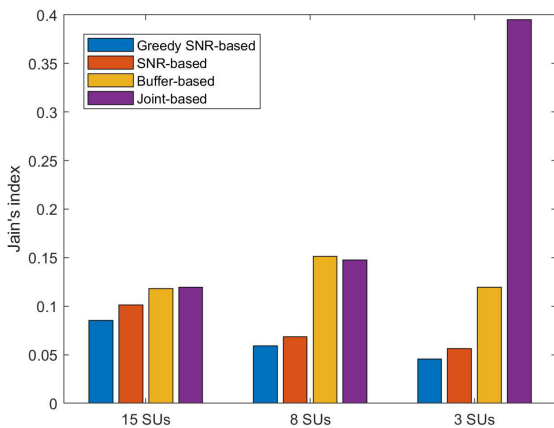
Figures 6(a), 6(b) and 6(c) show the effect of increasing the number of RBs on the average number of frames at the SUs' buffers. Figure 6, once again, shows that the SNR-based scheme is the worst in terms of the achieved buffer occupancies since it assigns resources on available channels to SUs that might not be underflowing while ignoring the buffer status of those suffering from underflow conditions. Specifically, allocation is completely done based on the reported SNR while disregarding the states of the playback buffers of the different SUs. On the other hand, it can be seen that the performance of the joint buffer and SNR-based scheme is comparable if not even better than the buffer-based scheme in almost all cases. This should be clear since the main objective



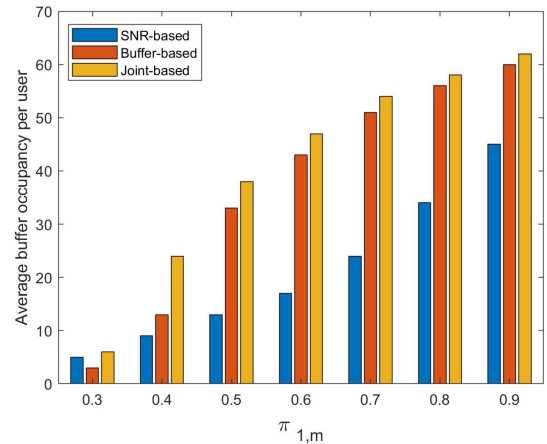
(a) Jain's index when a maximum of 6 RBs available.



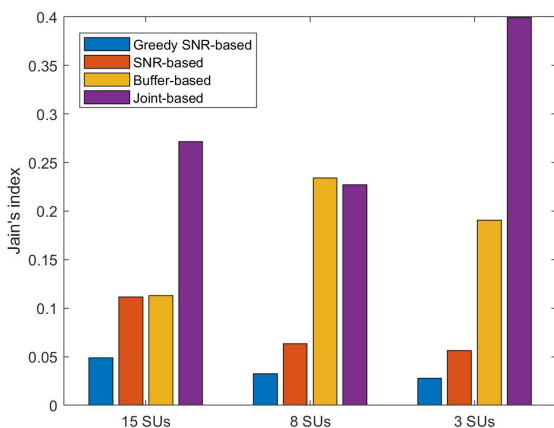
(a) SUs = 3.



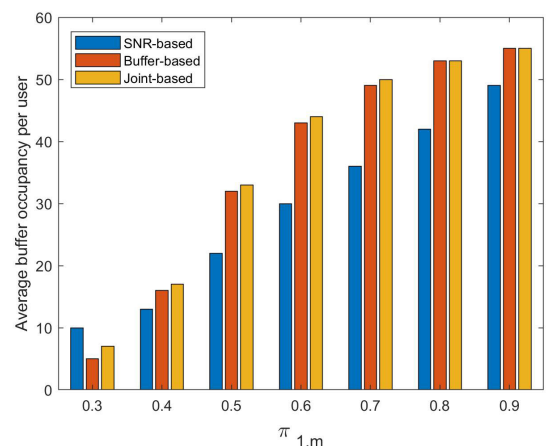
(b) Jain's index when a maximum of 15 RBs available.



(b) SUs = 8.



(c) Jain's index when a maximum of 25 RBs available.



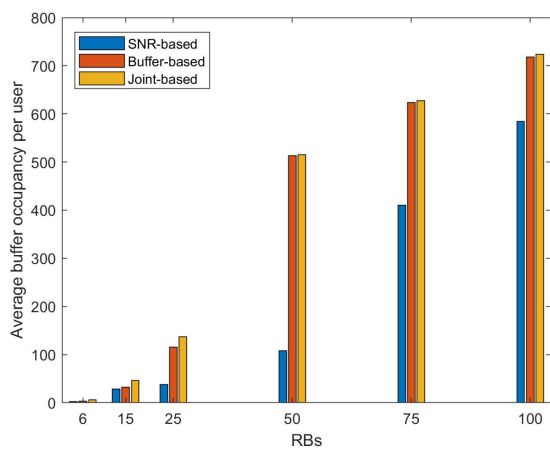
(c) SUs = 15.

**FIGURE 4.** Jain's index for greedy SNR, SNR, buffer, and joint buffer and SNR based allocation techniques vs. the number of active SUs for different number of available RBs.

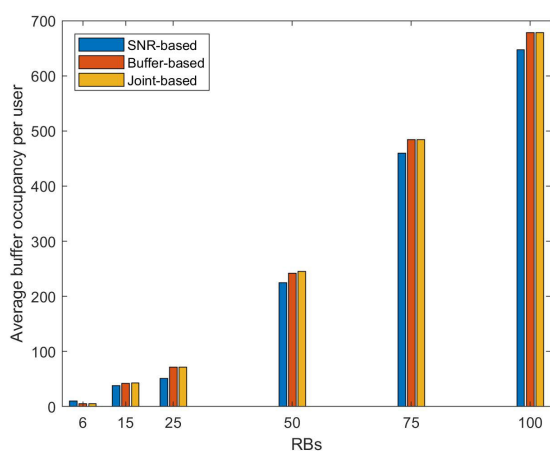
is met by maintaining a number of video frames at the SUs' buffers while taking into account the SNR as seen by the

**FIGURE 5.** The effect of probability of PUs' channels availability on the number of frames at the SUs' buffer.

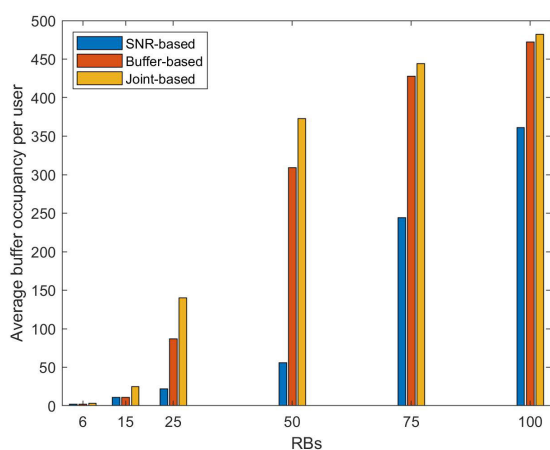
different SUs so as to guarantee efficient utilizations of the shared resources, which is reflected in the successful transmissions of the video frames. Another important observation



(a) SUs = 3.



(b) SUs = 8.



(c) SUs = 15.

**FIGURE 6.** The effect of the number of RBs on the average buffer occupancy per user.

is that as the number of the SUs increases from 3 to 15, the gap in performance between each of the schemes widens reflecting that the joint buffer and SNR-based outperforms

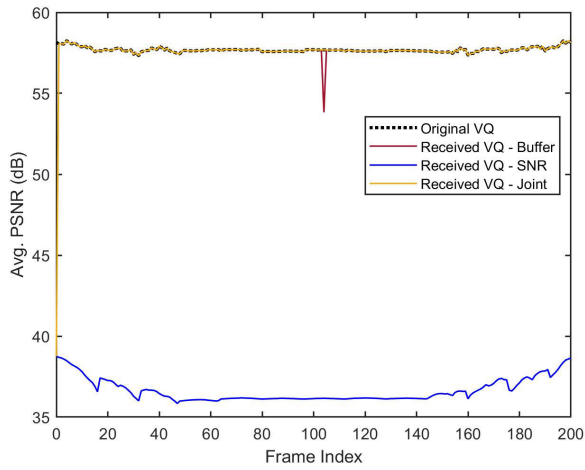
the other two schemes. It can also be noticed that the trend is more obvious when the maximum number of available RBs is small (e.g., 15 and 25) and becomes less obvious as the number of available RBs increases. This is simply explained by the fact that when the available resources are plenty there will almost be no compromises to make, and all the SUs in need will get the chance to meet their deadlines and avoid starvation in both schemes. On the other hand, when the number of available RBs is limited, the joint buffer and SNR-based outperforms the other schemes for the same reasons mentioned above.

**B. STREAMING OF SVC VIDEO**

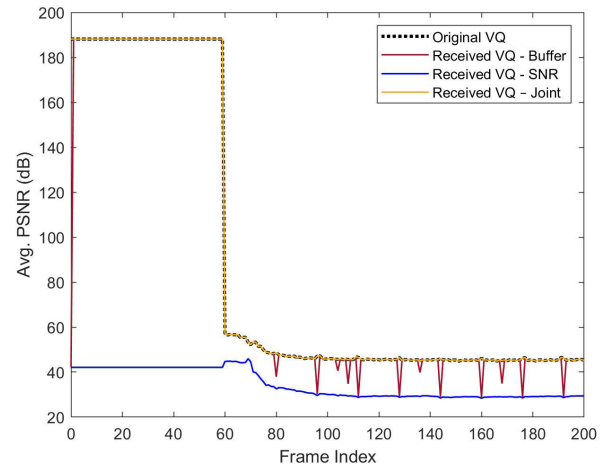
Similar to above, in this section, we study, compare and validate the proposed allocation and streaming strategies using MATLAB simulations averaged over 50 runs where each run lasts for 30 seconds. This is done assuming the same LTE structure as before and the same number of PUs and SUs while following the same transition matrices and limiting probability. However, the single layer H.264 encoded Sony Demo video sequence is now replaced with the Coarse-Grained video sequence (CGS) encoded Sony Demo video sequence, which consists of a BL and two ELs at a playback rate of  $f_p = 30$  fps. The peak signal-to-noise ratio (PSNR) metric will be used when comparing the performance of the three allocation methods. It is worth noting that in the previous discussion, the impact of the number of available RBs was highlighted, and the intuitive conclusion that increasing resources improves the streaming operation was further supported. Therefore, in this section, we only investigate two cases: operating at 20 MHz (i.e., the maximum number of available RBs is 100) and at 3 MHz (i.e., the maximum number of available RBs is 15). Buffer threshold ( $\Delta_{th}$ ) is set to 5 frames. Figure 7 shows the average PSNR of the received video for the case when the BS operates at 20 MHz assuming that the Sony Demo video sequence is transmitted to all SUs. Figures 7(a), 7(b), and 7(c) show that as the number of SUs increases from 3 to 15, the quality of the received video decreases since the share of each user from the available resources reduces as the number of SUs increase. Additionally, Figs. 7(a), 7(b), and 7(c) demonstrate that the SNR-based allocation scheme performs the worst similar to the conclusion in Section IV-A. This is also explained by the unfairness of the used algorithm where the available RBs are allocated based only on the channel quality as seen by the SUs irrespective of their buffer state and the urgency with which a frame should be received. Thus, available RBs may still be allocated to non-starving SUs as long as better channels are reported by these SUs for the available RBs. The figures also show that an average PSNR value of of 37 dB was achieved for the SNR-based allocation, which is the minimum PSNR among the three proposed allocation schemes. Such PSNR value is achieved as if only the base layer was received correctly.

In spite of the above, as will be shown later, some of the SUs were not allocated any RBs due to the poor reported CSI measured by those SUs. Figure 7(a) shows that, on average,

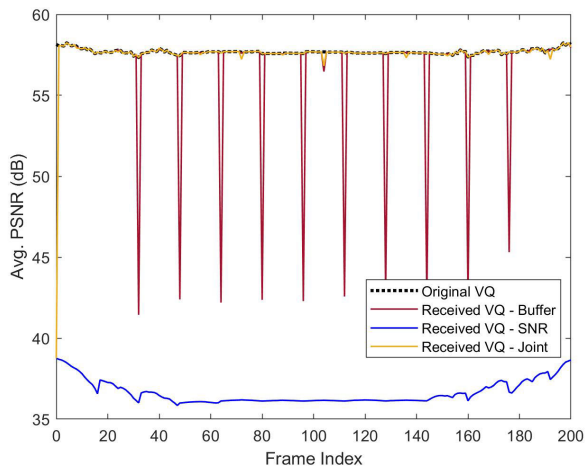




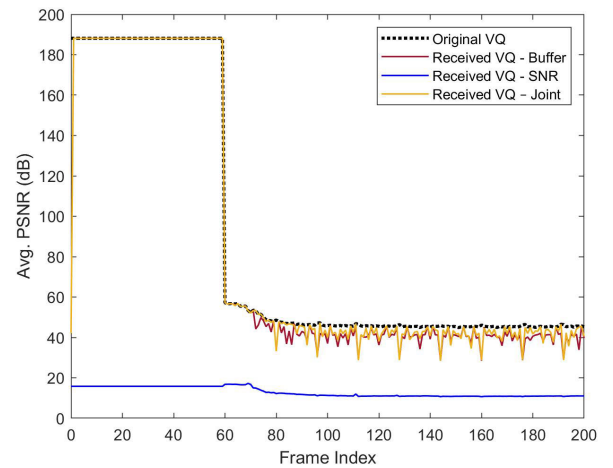
(a) SUs = 3.



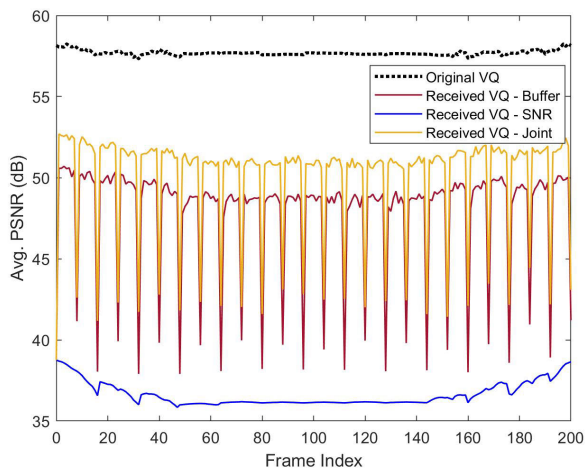
(a) SUs = 3.



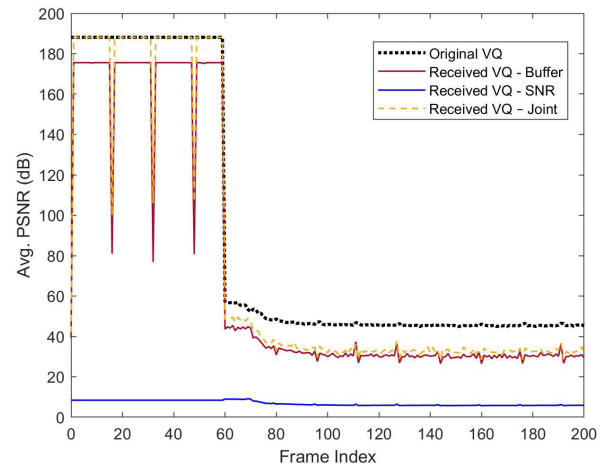
(b) SUs = 8.



(b) SUs = 8.



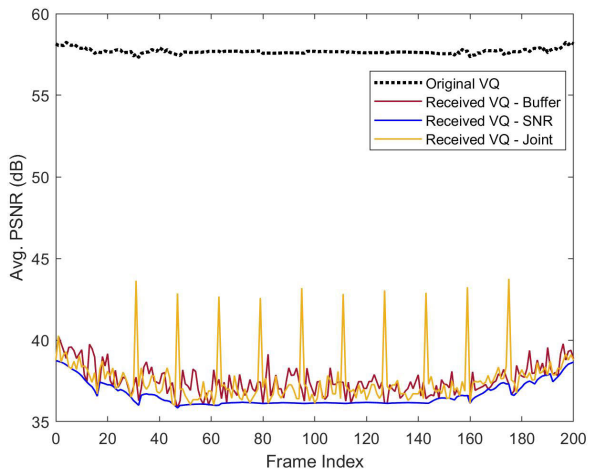
(c) SUs = 15.



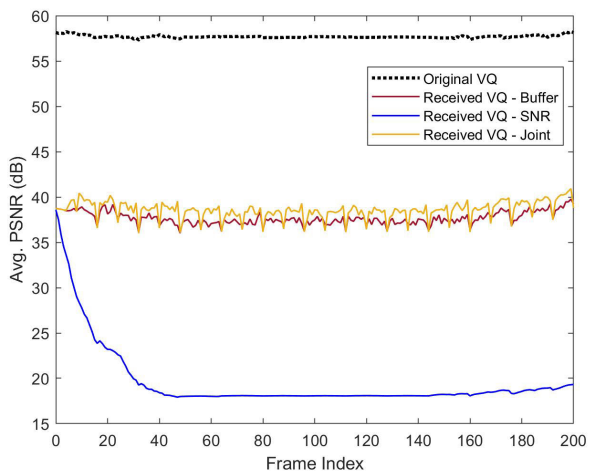
(c) SUs = 15.

**FIGURE 7.** Average PSNR when a maximum of 100 RBs (20 MHz) available (Sony Demo video sequences).

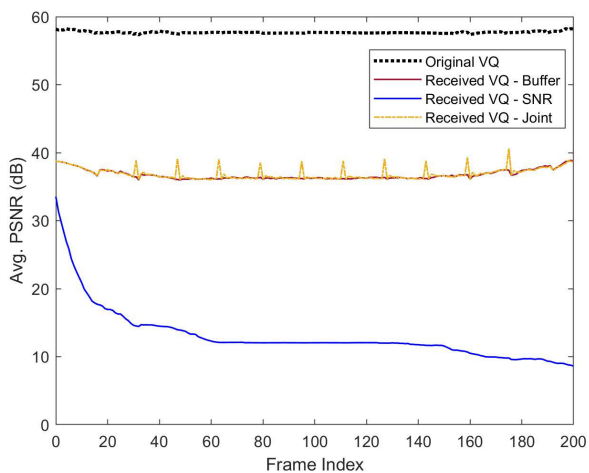
**FIGURE 8.** Average PSNR when a maximum of 100 RBs (20 MHz) available (Gandhi video sequences).



(a) SUs = 3.



(b) SUs = 8.



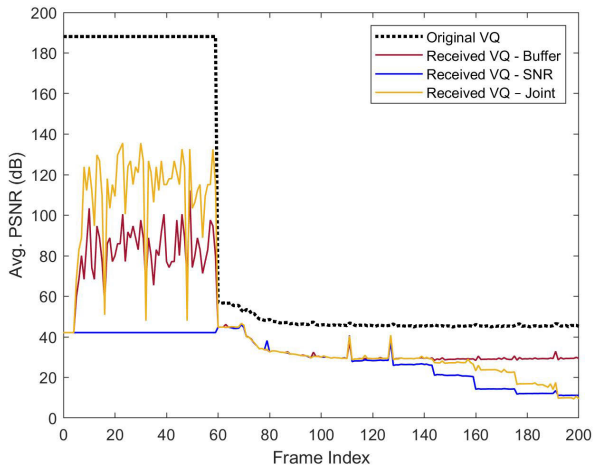
(c) SUs = 15.

**FIGURE 9.** Average PSNR when a maximum of 15 RBs (3 MHz) available (Sony Demo video sequences).

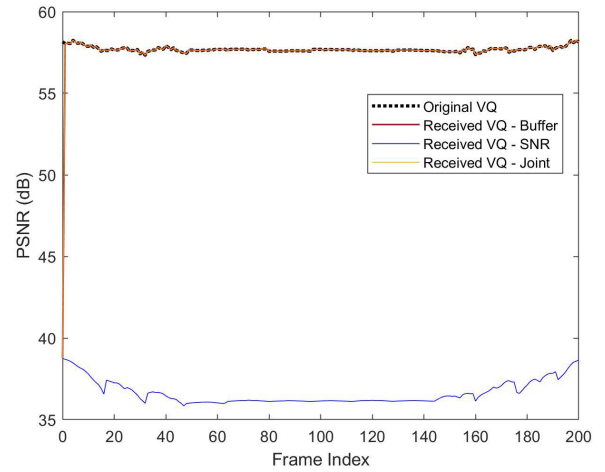
all SUs received the transmitted video sequence at the highest quality at a PSNR of 57 dB (i.e., received the BL and both of the ELs) when the joint buffer and SNR-based allocation scheme is used. Similar quality was achieved using the buffer-based allocation, but there was a slight drop in the quality at frame 100, which reflects that some SUs did not receive the two ELs due to the lack of available RBs at this time slot. Moreover, in Fig. 7(b), when the number of available SUs increases, the joint buffer and SNR-based clearly outperforms the buffer-based approach. There is also a noticeable degradation in the quality when the buffer-based allocation approach is used. Such degradation is attributed to the fact that the buffer-based approach serves the SUs with the lowest buffer occupancy first through random allocation of available RBs while ignoring the channel quality of the available RBs. Clearly, such allocation might not offer SUs in need with the RBs meeting their transmission rate requirements, which may cause starvation instants and interruptions in the playback process. On the other hand, this is not the case for the joint buffer and SNR-based approach as the buffer state and quality of RBs are considered when allocation is performed. Figure 7(c) shows the achieved average PSNR when the number of SUs is increased to 15 SUs. Although the buffer-based and joint buffer and SNR-based approaches have comparable performance, their performance shows that more SUs are able to receive frames with higher quality. This means that even when the number of RBs allocated to each SUs decreases due the increase of the number of SUs, the joint buffer and SNR-based allocation has better performance. It is important to note that sometimes the deep drops in the reconstructed quality of some of the frames is due to their large sizes (both the BL and ELs) and the situation is further aggregated when the time to transmit these big frames experiences limited available resources.

When the BS is operating at 20 MHz, Fig. 8 shows the average PSNR of the received video when the Ghandhi video sequences are transmitted to all SUs. Comparing Figs. 7 and 8, it is clear that both show similar trend. The joint buffer and SNR-based allocation scheme outperforms the other two schemes in most of the cases. Clearly, the figures also show that the SNR-based allocation scheme has the worst performance. It can also be noticed that the average PSNR decreases as the number of SUs increases for the case of SNR-based allocation, which was not the case when Sony Demo video sequence was used. The reason is that the Ghandhi video sequence has larger frame sizes because of its content. This is the reason that the minimum quality, which can be achieved by correctly receiving the BLs alone, was not achieved by some SUs, which is expected as the number of SUs is increased.

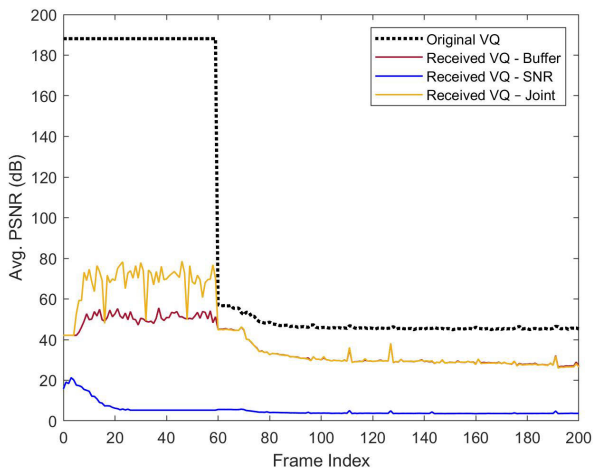
Figure 9 shows the average PSNR when the BS operates at 3 MHz (i.e., a maximum of 15 RBs available) and when the Sony Demo video sequence is transmitted to all SUs. Obviously, there is a great degradation in the quality of the



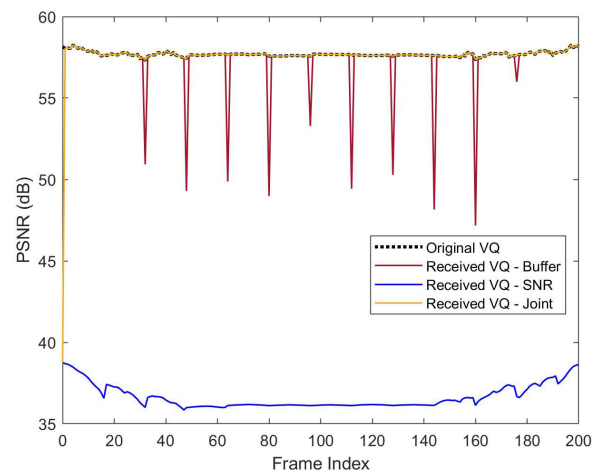
(a) SUs = 3.



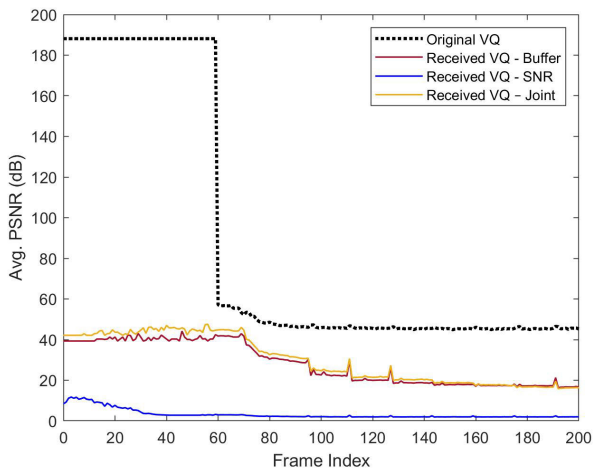
(a) SUs = 3.



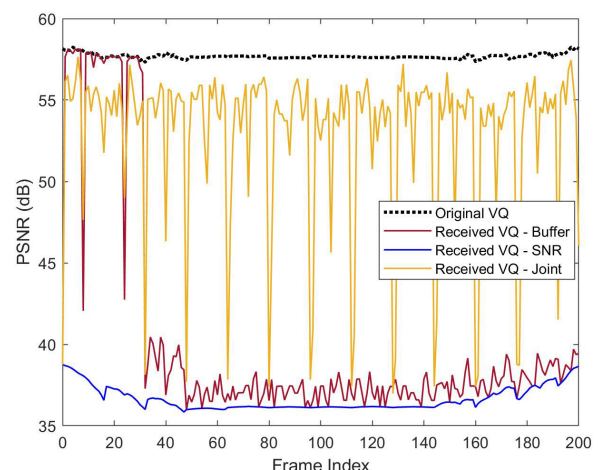
(b) SUs = 8.



(b) SUs = 8.



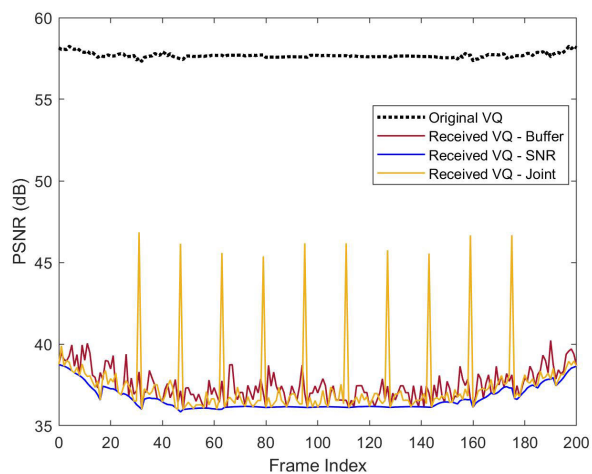
(c) SUs = 15.



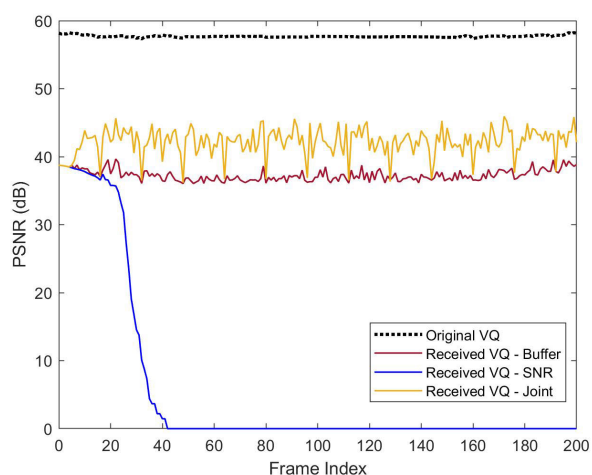
(c) SUs = 15.

FIGURE 10. Average PSNR when a maximum of 15 RBs (3 MHz) available (Gandhi video sequence).

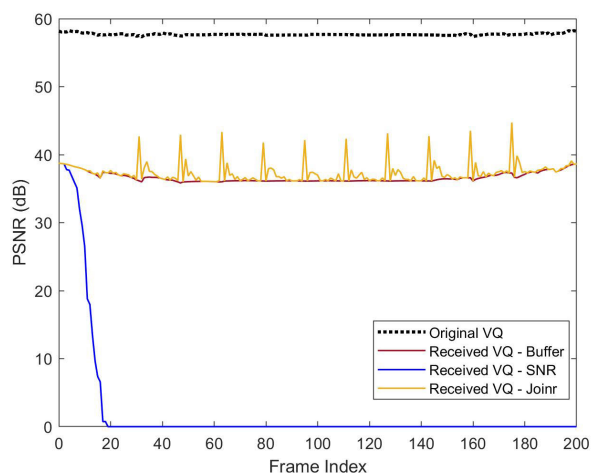
FIGURE 11. The PSNR of  $SU_2$  when a maximum of 100 RBs (20 MHz) available (Sony Demo video sequences).



(a) SUs = 3.



(b) SUs = 8.



(c) SUs = 15.

**FIGURE 12.** The PSNR of  $SU_2$  when a maximum of 15 RBs (3 MHz) available.

received video compared with Fig. 7, which is expected as the number of RBs decreases. Generally, the same trend occurs where the SNR-based approach has the worst performance and the joint buffer and SNR-based scheme performs the best. In Figs. 9(b) and 9(c), it can also be noticed that the SUs using the SNR-based allocation are suffering from huge degradation in the video quality since they do not even receive the BLs required to maintain the least acceptable quality. A reason for that is due to the limited number of available RBs for the SUs (15 RBs if all the 3 PU channels are idle and available). Clearly, in such a situation, contention among the SUs in need is increased. Another reason is due to the inherent unfairness of the algorithm itself as explained earlier. The buffer and joint allocation schemes are clearly of comparable performance. However, the joint buffer and SNR-based allocation scheme offers slightly better performance than the buffer-based one for the three scenarios. Finally, Figure 10 shows the average PSNR when the BS operates at 3 MHz for the Ghandhi video sequence. A similar trend to Fig. 9 is observed.

To study things more clearly, one of the SUs is further investigated to see how each of the allocation strategies performs from a user’s perspective and not on average as seen in the previous figures. To do so,  $SU_2$  is selected for further investigation when the Sony Demo video sequence is transmitted. Furthermore, we also monitored the changes experienced when more SUs joined the network for the three allocation schemes. As can be seen in Fig. 11(a),  $SU_2$  experiences similar behavior of smooth continuity at highest quality when the buffer-based and the joint buffer and SNR-based allocation schemes are used. On the other hand, when the SNR-based allocation scheme is used,  $SU_2$  can only receive the transmitted video sequence at its lowest quality, which is achieved by receiving only the BLs. Similar to before, as the number of contending SUs increases, the joint buffer and SNR-based allocation scheme outperforms the buffer-based allocation scheme as seen in Figs. 11(b) and 11(c). Figures 12(a), 12(b), and 12(c) show the video quality as received by  $SU_2$  when the BS operates at 3 MHz. Again, it can be seen that the joint buffer and SNR-based allocation scheme achieves a better reconstructed video quality at  $SU_2$ . Also, Figures 12(b) and (c) explain the degradation in the average quality as seen in Figs. 9(a) and 9 (b), as  $SU_2$  is only able to receive 20 frames for the case of 8 active SUs and 40 frames for 15 active SUs. This shows that some SUs might not be able to receive the video sequence fully and thus suffer from unavoidable starvation instants causing unpleasant interruptions in the playback process. Such situations are not happening in the case when the joint buffer and SNR-based approach is used, which always outperforms the SNR-based approach for all the scenarios.

**V. CONCLUSION**

In this paper, we proposed and compared the performance of three allocation strategies to efficiently share available

resources between contending secondary users (SUs) in an LTE-based CR network. The proposed allocation approaches are SNR-based, buffer-based, and joint buffer and SNR-based schemes. The performance of the proposed schemes was compared in the context of video streaming. Therefore, the main objective is to stream the video sequences to the different SUs while guaranteeing continuous playback at acceptable perceptual quality. In addition, to better achieve this goal, a scalable video coding (SVC) technique is applied to adapt to the dynamic availability of the primary channels. SVC is employed to enhance the quality of the received video sequences by adapting the transmission process to the changing resources and improving the achieved video quality by transmitting the enhancement layers of transmitted video frames only when possible (i.e., when the conditions set by the streaming algorithm are met). Clearly, the proposed approach exhibits a relatively low complexity when compared to other approaches. This is attributed to the fact the proposed approach does not require any reconfiguration for the codec parameters. The proposed allocation algorithms adaptively assign available RBs to SUs in need while considering the quality of their assigned channels as well as their buffer occupancies. This is all done while guaranteeing the reception of the video frames within their deadlines. Simulation results show that the joint buffer and SNR-based algorithm outperforms the other two algorithms even under limited resources and even when the number of active SUs increases.

## ACKNOWLEDGMENT

This paper represents the opinions of the author(s) and does not mean to represent the position or opinions of the American University of Sharjah.

## REFERENCES

- [1] S. Jose, *Cisco Visual Networking Index: Forecast and Trends, 2017–2022*, Cisco Syst., San Jose, CA, USA, 2018.
- [2] *2020 Global Networking Trends Report, 2017–2022*, Cisco Syst., San Jose, CA, USA, 2020.
- [3] FCC, *Spectrum Policy Task Force*, ET Docket 02–135, Nov. 2002.
- [4] W. Yin and H. Chen, “Decision-driven time-adaptive spectrum sensing in cognitive radio networks,” *IEEE Trans. Wireless Commun.*, vol. 19, no. 4, pp. 2756–2769, Apr. 2020.
- [5] S. Geirhofer, L. Tong, and B. M. Sadler, “Cognitive medium access: Constraining interference based on experimental models,” *IEEE J. Sel. Areas Commun.*, vol. 26, no. 1, pp. 95–105, Jan. 2008.
- [6] J. Mitola, “Cognitive radio for flexible mobile multimedia communications,” in *Proc. IEEE Int. Workshop Mobile Multimedia Commun. (MoMuC)*, Nov. 1999, pp. 435–441.
- [7] R. Tandra, S. M. Mishra, and A. Sahai, “What is a spectrum hole and what does it take to recognize one?” *Proc. IEEE*, vol. 97, no. 5, pp. 824–848, May 2009.
- [8] H. P. Shiang and M. van der Schaar, “Queuing-based dynamic channel selection for heterogeneous multimedia applications over cognitive radio networks,” *IEEE Trans. Multimedia*, vol. 10, no. 5, pp. 896–909, Aug. 2008.
- [9] S.-Y. Lien, K.-C. Chen, Y.-C. Liang, and Y. Lin, “Cognitive radio resource management for future cellular networks,” *IEEE Wireless Commun.*, vol. 21, no. 1, pp. 70–79, Feb. 2014.
- [10] S. Sesia, I. Toufik, and M. Baker, *LTE-the UMTS Long Term Evolution: From Theory to Practice*. Hoboken, NJ, USA: Wiley, 2011.
- [11] *Physical Layer Procedures*, 3GPP document TS 36.213, 3GPP TR Release 13, 2016. [Online]. Available: [https://www.etsi.org/deliver/etsi\\_ts/136200\\_136299/136213/13.00.00\\_60/ts\\_136213v130000p.pdf](https://www.etsi.org/deliver/etsi_ts/136200_136299/136213/13.00.00_60/ts_136213v130000p.pdf)
- [12] A. Asheralieva and K. Mahata, “Resource allocation for LTE-based cognitive radio network with queue stability and interference constraints,” *Phys. Commun.*, vol. 14, pp. 1–13, Mar. 2015.
- [13] B. Kouassi, L. Deneire, B. Zayen, R. Knopp, F. Kalteneberger, F. Negro, D. Stock, and I. Ghaur, “Design and implementation of spatial interweave LTE-TDD cognitive radio communication on an experimental platform,” *IEEE Wireless Commun.*, vol. 20, no. 2, pp. 60–67, Apr. 2013.
- [14] J. D. Naranjo, I. Viering, and K.-J. Friederichs, “A cognitive radio based dynamic spectrum access scheme for LTE heterogeneous networks,” in *Proc. Wireless Telecommun. Symp.*, Apr. 2012, pp. 1–7.
- [15] E. Z. Tragos, S. Zeadally, A. G. Fragkiadakis, and V. A. Siris, “Spectrum assignment in cognitive radio networks: A comprehensive survey,” *IEEE Commun. Surveys Tuts.*, vol. 15, no. 3, pp. 1108–1135, 3rd Quart., 2013.
- [16] A. E. Omer, M. S. Hassan, and M. El-Tarhuni, “An integrated scheme for streaming scalable encoded video-on-demand over CR networks,” *Phys. Commun.*, vol. 35, Aug. 2019, Art. no. 100701.
- [17] A. E. Omer, M. S. Hassan, and M. El-Tarhuni, “Window-based adaptive technique for real-time streaming of scalable video over cognitive radio networks,” *IET Commun.*, vol. 11, no. 17, pp. 2643–2649, 2017.
- [18] S. Dey and I. S. Misra, “Content driven proportionate channel allocation scheme for scalable video over cognitive radio network,” in *Proc. IEEE Calcutta Conf. (CALCON)*, Feb. 2020, pp. 59–63.
- [19] H. B. Salameh and R. Abusamra, “Intelligent multicast routing for multimedia over cognitive radio networks: A probabilistic approach,” *Multimedia Tools Appl.*, vol. 1, no. 1, pp. 1–12, 2020.
- [20] M. Bkassiny and S. K. Jayaweera, “Optimal channel and power allocation for secondary users in cooperative cognitive radio networks,” in *Proc. Int. Conf. Mobile Lightweight Wireless Syst.*, 2010, pp. 180–191.
- [21] H. B. Salameh, M. Krunz, and O. Younis, “Distance-and traffic-aware channel assignment in cognitive radio networks,” in *Proc. 5th Annu. IEEE Commun. Soc. Conf. Sensor, Mesh Ad Hoc Commun. Netw.*, Jun. 2008, pp. 10–18.
- [22] M. Khabazian, S. Aissa, and N. Tadayon, “Performance modeling of a two-tier primary-secondary network operated with IEEE 802.11 DCF mechanism,” *IEEE Trans. Wireless Commun.*, vol. 11, no. 9, pp. 3047–3057, Sep. 2012.
- [23] W. Y. Lee and I. F. Akyildiz, “Optimal spectrum sensing framework for cognitive radio networks,” *IEEE Trans. Wireless Commun.*, vol. 7, no. 10, pp. 3845–3857, Oct. 2008.
- [24] Y. Chen, Q. Zhao, and A. Swami, “Joint design and separation principle for opportunistic spectrum access in the presence of sensing errors,” *IEEE Trans. Inf. Theory*, vol. 54, no. 5, pp. 2053–2071, May 2008.
- [25] A. A. Daoud, M. Alanyali, and D. Starobinski, “Secondary pricing of spectrum in cellular CDMA networks,” in *Proc. 2nd IEEE Int. Symp. New Frontiers Dyn. Spectr. Access Netw.*, Apr. 2007, pp. 535–542.
- [26] C. T. Chou, S. S. N. H. Kim, and K. G. Shin, “What and how much to gain by spectrum agility?” *IEEE J. Sel. Areas Commun.*, vol. 25, no. 3, pp. 576–588, Apr. 2007.
- [27] B. Canberk, I. F. Akyildiz, and S. Oktug, “Primary user activity modeling using first-difference filter clustering and correlation in cognitive radio networks,” *IEEE/ACM Trans. Netw.*, vol. 19, no. 1, pp. 170–183, Feb. 2011.
- [28] I. Suliman, J. Lehtomaki, T. Braysy, and K. Umehayashi, “Analysis of cognitive radio networks with imperfect sensing,” in *Proc. IEEE 20th Int. Symp. Pers., Indoor Mobile Radio Commun.*, Sep. 2009, pp. 1616–1620.
- [29] B. Wang, Z. Ji, K. J. R. Liu, and T. C. Clancy, “Primary-prioritized Markov approach for dynamic spectrum allocation,” *IEEE Trans. Wireless Commun.*, vol. 8, no. 4, pp. 1854–1865, Apr. 2009.
- [30] Y. Yao, Z. Feng, and D. Miao, “Markov-based optimal access probability for dynamic spectrum access in cognitive radio networks,” in *Proc. IEEE 71st Veh. Technol. Conf.*, May 2010, pp. 1–5.
- [31] Y. Aborahama and M. S. Hassan, “On the stochastic modeling of the holding time of SUs to PU channels in cognitive radio networks,” *IEEE Trans. Cognit. Commun. Netw.*, vol. 6, no. 1, pp. 282–295, Mar. 2020.
- [32] Y. Abo Rahama, M. S. Hassan, and M. H. Ismail, “A stochastic-based rate control approach for video streaming over cognitive radio networks,” *IEEE Trans. Cognit. Commun. Netw.*, vol. 5, no. 1, pp. 181–192, Mar. 2019.
- [33] S. N. Shankar, C.-T. Chou, K. Challapali, and S. Mangold, “Spectrum agile radio: Capacity and QoS implications of dynamic spectrum assignment,” in *Proc. IEEE Global Telecommun. Conf. (GLOBECOM)*, Nov./Dec. 2005, p. 2516.

- [34] M. Derakhshani and T. Le-Ngoc, "Learning-based opportunistic spectrum access with adaptive hopping transmission strategy," *IEEE Trans. Wireless Commun.*, vol. 11, no. 11, pp. 3957–3967, Nov. 2012.
- [35] S. Bayhan and F. Alagöz, "A Markovian approach for best-fit channel selection in cognitive radio networks," *Ad Hoc Netw.*, vol. 12, pp. 165–177, Jan. 2014.
- [36] M. Helmy, Y. Aborahama, M. S. Hassan, and M. H. Ismail, "A probabilistic closed-form expression for the amount of data secondary users can transmit in cognitive radio networks," in *Proc. Wireless Telecommun. Symp. (WTS)*, Apr. 2019, pp. 1–5.
- [37] Y. Saleem and M. H. Rehmani, "Primary radio user activity models for cognitive radio networks: A survey," *J. Netw. Comput. Appl.*, vol. 43, pp. 1–16, Aug. 2014.
- [38] R. L. Batista, C. F. M. Silva, T. F. Maciel, J. M. B. Silva, and F. R. P. Cavalcanti, "Joint opportunistic scheduling of cellular and device-to-device communications," *J. Commun. Inf. Syst.*, vol. 32, no. 1, pp. 62–73, 2017.
- [39] F. Li, P. Ren, and Q. Du, "Joint packet scheduling and subcarrier assignment for video communications over downlink OFDMA systems," *IEEE Trans. Veh. Technol.*, vol. 61, no. 6, pp. 2753–2767, Jul. 2012.
- [40] Y. Zhang and G. Liu, "Fine granularity resource allocation algorithm for video transmission in orthogonal frequency division multiple access system," *IET Commun.*, vol. 7, no. 13, pp. 1383–1393, Sep. 2013.
- [41] E. Axell, G. Leus, E. Larsson, and H. Poor, "Spectrum sensing for cognitive radio: State-of-the-art and recent advances," *IEEE Signal Process. Mag.*, vol. 29, no. 3, pp. 101–116, May 2012.
- [42] H. Xing and S. Hakola, "The investigation of power control schemes for a device-to-device communication integrated into OFDMA cellular system," in *Proc. 21st Annu. IEEE Int. Symp. Pers., Indoor Mobile Radio Commun.*, Sep. 2010, pp. 1775–1780.



**MARAM HELMY** received the bachelor's degree (*summa cum laude*) in electronics and communication engineering from the American University of Ras Al Khaimah, in 2016, and the M.Sc. degree in electrical engineering from the American University of Sharjah, in 2020. In 2017, she worked as a Research Assistant with the American University of Ras Al Khaimah. In 2018, she joined the Electrical Engineering Master's Program with the American University of Sharjah, where she was granted a graduate teaching assistantship. She coauthored of three conference papers and one journal. Her research interests include multimedia streaming, wireless communications, digital signal processing, and machine learning.



**MOHAMED S. HASSAN** received the M.Sc. degree in electrical engineering from the University of Pennsylvania, Philadelphia, in 2000, and the Ph.D. degree in electrical and computer engineering from the University of Arizona, USA, in 2005. He is currently a Full Professor in electrical engineering with the American University of Sharjah. Recently, he was involved in multiple projects related to free space optical communications, electromagnetic shielding, demand response & smart grids, anti-static flooring, and fiber optic sensors for infrastructure health monitoring applications. His research interests include multimedia communications and networking, wireless communications, cognitive radios, resource allocation and performance evaluation of wired & wireless networks, and next generation wireless systems.



**MAHMOUD H. ISMAIL** (Senior Member, IEEE) received the B.Sc. degree (Hons.) in electronics and electrical communications engineering and the M.Sc. degree in communications engineering from Cairo University, Egypt, in 2000 and 2002, respectively, and the Ph.D. degree in electrical engineering from The University of Mississippi, MS, USA, in 2006. From August 2000 to August 2002, he was a Research and Teaching Assistant with the Department of Electronics and Electrical Communications Engineering, Cairo University. From 2004 to 2006, he was a Research Assistant with the Center for Wireless Communications (CWC), The University of Mississippi. He is currently a Full Professor (on leave) with the Department of Electronics and Electrical Communications Engineering, Cairo University, and an Associate Professor with the American University of Sharjah, Sharjah, United Arab Emirates. He was also a Systems Engineering Consultant at Newport Media Inc., (currently part of Microchip), Egypt Design Center, Cairo, from 2006 to 2014. His research interests include general area of wireless communications with emphasis on performance evaluation of next-generation wireless systems and communications over fading channels. He is a member of Sigma Xi and Phi Kappa Phi. He was a recipient of The University of Mississippi Summer Assistantship Award, in 2004 and 2005, The University of Mississippi Dissertation Fellowship Award, in 2006, The University of Mississippi Graduate Achievement Award in Electrical Engineering, in 2006, and the Best Paper Award presented at the 10th IEEE Symposium on Computers and Communications (ISCC 2005), La Manga del Mar Menor, Spain. He served as a reviewer for several refereed journals and conferences.

...